Uniform thermal expansion reactivity evaluation based on reactivity coefficient for sodium-cooled fast reactor

Satoshi Takeda[1]
Osaka University
Osaka, Suita, Yamadaoka 2-1, Japan
e-mail: takeda@see.eng.osaka-u.ac.jp

Takanori Kitada
Osaka University
Osaka, Suita, Yamadaoka 2-1, Japan
e-mail: kitada@see.eng.osaka-u.ac.jp

Takafumi Okita
Osaka University
Osaka, Suita, Yamadaoka 2-1, Japan
e-mail: okita@see.eng.osaka-u.ac.jp

Eiji Hoashi
Osaka University
Osaka, Suita, Yamadaoka 2-1, Japan
e-mail: hoashi@see.eng.osaka-u.ac.jp

ABSTRACT

This paper presents a method for calculating reactivity changes caused by uniform thermal expansion in sodium-cooled fast reactors using reactivity coefficients. The reactivity changes due to both Z-axis and radial expansion are separated into two effects: the shape change effect and the macroscopic cross-section change effect. These effects are expressed using the reactivity coefficients of materials in the reactor core. The reactivity change due to Z-axis expansion considers the expansion of the fuel, cladding, and wrapper tube, while the radial expansion considers the fuel pin, structural materials, and reactor core support structures. To confirm the accuracy of this approach, calculations were performed for simplified reactor geometry with different height-to-diameter ratios. The results show that reactivity changes behave almost linearly for expansions of up to 2%. Additionally, the difference between the expansion reactivity obtained by using reactivity coefficients and those by direct calculations considering core expansion is within a few percent.

[1] Corresponding author.

1 Introduction

Various types of sodium-cooled fast reactors have been studied, and it is known that the nuclear characteristics, such as sodium void reactivity, differ significantly depending on the reactor design [1-5]. Therefore, in the design of fast reactors, transient analysis is generally performed to ensure core safety during accidents such as unprotected transient overpower [6,7]. In transient analysis of severe accidents for a fast reactor, it is important to evaluate the reactivity introduced by the expansion of the core and changes in fuel and coolant temperatures. In the neutron transport calculation, the reactivity feedback introduced by changes in fuel and coolant temperature can be accounted for by using cross sections corresponding to the transient conditions. However, the geometric change caused by the expansion of the core requires a separate evaluation from neutron transport calculations. A direct approach to account for geometric changes is the coupling of neutron transport calculation with structural analysis codes. Directly accounting for geometric changes in neutron transport calculations requires performing neutron transport calculations for continuously changing geometry. As a result, the computational time increases significantly. Therefore, it is effective to evaluate expansion reactivity based on reactivity coefficients in core design.

A method that uses reactivity coefficients to account for the assembly bowing due to changes in the temperature distribution within the fuel assemblies has been proposed [8,9]. This method is based on the perturbation theory, and the verification was conducted using Monte Carlo calculations [9]. In addition to the assembly bowing, there are expansions, such as the vertical expansion of the reactor core due to increased fuel

temperature, and the expansion of reactor core support plates due to the increase in inlet coolant temperature, which are significant in the analysis of the fast reactor Monju [7]. For sodium-cooled fast reactors using oxide fuels, formulas for calculating these expansion reactivities are provided [10]. However, the assumptions used in deriving the reactivity evaluation formula based on reactivity coefficients, and the approximation errors have not been sufficiently discussed.

In our previous study [11], as part of verification of calculations using reactivity coefficients, we evaluated an error due to reactivity component separation using the Monte Carlo code MVP [12]. However, the results include statistical errors, and the calculation did not utilize reactivity coefficients. Therefore, in this paper, the aim is to evaluate the accuracy of calculations using reactivity coefficients by using the diffusion theory code CITATION [13]. In this study, to conduct an fundamental investigation of expansion reactivity based on reactivity coefficients, we assume that the core expands uniformly in the Z-axis or radial direction, and non-uniform expansions, such as bowing, are left for future work. Section 2 presents the derivation of Z-axis expansion reactivity using reactivity coefficients. Section 3 presents the derivation of radial expansion reactivity. Section 4 shows the differences from formulas derived in previous study [10]. Section 5 discusses the errors in calculations using reactivity coefficients. Section 6 presents the conclusions.

2 Derivation of Z-axis expansion reactivity

In this study, the shape change effect is defined as the reactivity introduced due to a change in the reactor core height while keeping the macroscopic cross-section constant. The macroscopic cross-section change effect is defined as the reactivity introduced due to a change in the macroscopic cross-section while keeping the reactor core height constant. The total reactivity inserted when the core expands along Z-axis can be approximately separated into the shape change effect and the macroscopic cross-section change effect as

$$\rho_z = \frac{\{k(H',\Sigma') - k(H,\Sigma)\}}{k(H',\Sigma')k(H,\Sigma)} \approx \rho_{z,S} + \rho_{z,\Sigma}, \quad (1)$$

where, H and H' represent the core height before and after expansion, respectively, and Σ and Σ' are the macroscopic cross-sections before and after expansion. The term $\rho_{z,S} = \frac{k(H',\Sigma)-k(H,\Sigma)}{k(H',\Sigma)k(H,\Sigma)}$ represents the geometric change effect, while $\rho_{z,\Sigma} = \frac{k(H,\Sigma')-k(H,\Sigma)}{k(H,\Sigma')k(H,\Sigma)}$ represents the macroscopic cross-section change effect.

The reactivity change due to the variation in core height can be expressed as:

$$\rho_{z,S} = K_H \frac{\Delta H}{H}, \quad (2)$$

where ΔH is the change in core height and K_H is the reactivity coefficient of core height. By representing the core height with the height of the fuel section, the expression becomes

$$\rho_{z,S} = K_H \frac{\Delta H_f}{H_f}, \quad (3)$$

where subscript f represents the fuel. Using the linear thermal expansion coefficient, the relative change in the core height direction is given by

$$\frac{\Delta H_f}{H_f} = \alpha_f \Delta T_f, \tag{4}$$

where α_f is the linear thermal expansion coefficient of the fuel, and ΔT_f is the fuel temperature change. Then, the shape change effect can be described as:

$$\rho_{z,s} = K_H \alpha_f \Delta T_f. \tag{5}$$

Moving on to $\rho_{z,\Sigma}$, since changes in the macroscopic cross-section can be represented by density changes, the reactivity introduced by density changes is decomposed as

$$\rho_{z,\Sigma} = \sum_i \frac{\partial keff}{\partial d_i/d_i} \frac{\partial d_i/d_i}{\partial H_i/H_i} \frac{\Delta H_i}{H_i}, \tag{6}$$

where d_i and H_i represent the density and the height of material i (fuel, cladding, or wrapper tube). Then we introduce the density reactivity coefficient described as

$$K_{d,i} = \frac{\partial keff}{\partial d_i/d_i}. \tag{7}$$

In addition, we use an approximation of:

$$\frac{\partial d_i/d_i}{\partial H_i/H_i} \approx -1. \tag{8}$$

Using Eqs. (7) and (8), Eq. (6) can be rewritten as

$$\rho_{z,\Sigma} = -\sum_i K_{d,i} \alpha_i \Delta T_i. \tag{9}$$

y summing $\rho_{z,s}$ and $\rho_{z,\Sigma}$, the Z-axis expansion reactivity is described as:

$$\rho_z = K_H \alpha_f \Delta T_f - \sum_i K_{d,i} \alpha_i \Delta T_i = \left(K_H - K_{d,f}\right) \alpha_f \Delta T_f - K_{d,cl} \alpha_{cl} \Delta T_{cl} - K_{d,wr} \alpha_{wr} \Delta T_{wr}, \tag{10}$$

where, subscript cl and wr represents the cladding and wrapper tube, respectively. In Eq. (10), the reactivity associated with the thermal expansion of the wrapper tube is also

included, but in events where the fuel temperature changes significantly, this reactivity becomes relatively small.

3 Derivation of radial expansion reactivity

The radial expansion considered in the present study includes the expansion of the reactor core support plates at the bottom of the core, which leads to an increase in the coolant flow paths, and the radial expansion of fuel pins which involves the fuel-cladding interaction. While the interaction depends on the fuel material and its burnup, the fuel pellet and cladding are collectively considered as one region in the derivation. Similar to z-axis expansion reactivity, the radial expansion reactivity is approximately separated into the shape change effect and the macroscopic cross-section change effect as

$$\rho_r = \frac{\{keff(R',\Sigma') - keff(R,\Sigma)\}}{keff(R',\Sigma')keff(R,\Sigma)} \approx \rho_{r,s} + \rho_{r,\Sigma}, \tag{11}$$

Here, R and R' represent the core radius before and after expansion, respectively. The term $\rho_{r,s} = \frac{keff(R',\Sigma) - keff(R,\Sigma)}{keff(R',\Sigma)keff(R,\Sigma)}$ represents the geometric change effect, while $\rho_{r,\Sigma} = \frac{keff(R,\Sigma') - keff(R,\Sigma)}{keff(R,\Sigma')keff(R,\Sigma)}$ represents the macroscopic cross-section change effect.

Let us consider a situation that the lower core support plate expands, leading to the radial expansion of the reactor core. The reactivity $\rho_{r,s}$ can be described by introducing the core radial reactivity coefficient as

$$\rho_{r,s} = K_R \frac{\Delta A_{support}}{A_{support}} = 2K_R \left(\left(1 + \alpha_{support} \Delta T_{support}\right)^2 - 1 \right) \tag{12}$$

$$\approx 2K_R\alpha_{support}\Delta T_{support},$$

where A is the area, K_R is the reactivity coefficient of core radial, and subscript $support$ represents the core support plate. Since the expansion ratio is generally less than a few percent, the term $\left(\alpha_{support}\Delta T_{support}\right)^2$ becomes negligible and the approximation is justified.

Next, we consider the reactivity $\rho_{r,\Sigma}$ due to changes in the macroscopic cross-section. The changes in macroscopic cross-section can be represented by changes in density, thus we consider the densities of the fuel pin, structural materials such as wrapper tubes, and coolant. Since the total mass of the fuel pin and structural materials does not change after the expansion, we obtain

$$\frac{\Delta d_{p,homo}}{d_{p,homo}} = \frac{\Delta d_{s,homo}}{d_{s,homo}} = \frac{V_t}{V_t'} - 1 \approx -\frac{\Delta V_t}{V_t}. \tag{13}$$

where $d_{p,homo}$ and $d_{s,homo}$ are the homogenized densities of the fuel pin and structural materials, respectively, and V_t and V_t' are the total volumes before and after expansion. The change in homogenized coolant density of the core can be expressed as

$$\begin{aligned}\Delta d_{c,homo} &= \frac{d_{c,homo}V_t + d_c\Delta V_c}{V_t'} - d_{c,homo} \\ &= \frac{d_{c,homo}V_t + d_c\left(\Delta V_t - \Delta V_p - \Delta V_s\right)}{V_t'} - d_{c,homo} \\ &= \frac{-d_{c,homo}\Delta V_t + d_c\left(\Delta V_t - \Delta V_p - \Delta V_s\right)}{V_t'}.\end{aligned} \tag{14}$$

where subscript c represents the coolant. In Eq. (14), we use a relationship of

$$\Delta V_t = \Delta V_p + \Delta V_s + \Delta V_c. \tag{15}$$

Next, the following relationship is utilized:

$$d_c = d_{c,homo}\frac{V_t}{V_c}. \tag{16}$$

Using Eq. (16), Eq. (14) becomes

$$\begin{aligned}\Delta d_{c,homo} &= d_{c,homo}\frac{\Delta V_t}{V_t}\left(-1+\frac{V_t}{V_c}\right) - d_{c,homo}\frac{\Delta V_p + \Delta V_s}{V_c} \\ &= d_{c,homo}\frac{\Delta V_t}{V_t}\left(\frac{V_p + V_s}{V_c}\right) - d_{c,homo}\frac{\Delta V_p + \Delta V_s}{V_c}.\end{aligned} \tag{17}$$

Hence, the relative change in $d_{c,homo}$ is described as

$$\frac{\Delta d_{c,homo}}{d_{c,homo}} = \frac{\Delta V_t}{V_t}\left(\frac{V_p + V_s}{V_c}\right) - \frac{\Delta V_p + \Delta V_s}{V_c}. \tag{18}$$

The reactivity introduced by relative density changes is obtained by multiplying by the density reactivity coefficients as

$$\begin{aligned}\rho_{r,\Sigma} &= K_{d,p}\frac{\Delta d_{p,homo}}{d_{p,homo}} + K_{d,s}\frac{\Delta d_{s,homo}}{d_{s,homo}} + K_{d,c}\frac{\Delta d_{c,homo}}{d_{c,homo}} \\ &= -K_{d,p}\frac{\Delta V_t}{V_t} - K_{d,s}\frac{\Delta V_t}{V_t} + K_{d,c}\frac{\Delta V_t}{V_t}\left(\frac{V_p + V_s}{V_c}\right) - K_{d,c}\frac{\Delta V_p}{V_c} - K_{d,c}\frac{\Delta V_s}{V_c},\end{aligned} \tag{19}$$

where, $K_{d,p}$, $K_{d,s}$, and $K_{d,c}$ the density reactivity coefficients of fuel pin, structural materials, and coolant. Using the following relationships:

$$\frac{\Delta V_t}{V_t} = 2\alpha_{support}\Delta T_{support} \tag{20}$$

$$\frac{\Delta V_p}{V_p} = 2\alpha_p \Delta T_p \tag{21}$$

$$\frac{\Delta V_s}{V_s} = 2\alpha_s \Delta T_s \tag{22}$$

we can rewrite $\rho_{r,\Sigma}$ as

$$\rho_{r,\Sigma} = 2\alpha_{support}\Delta T_{support}\left(K_{d,c}\frac{V_p + V_s}{V_c} - \left(K_{d,p} + K_{d,s}\right)\right) - 2\alpha_p \Delta T_p K_{d,c}\frac{V_p}{V_c} \tag{23}$$

$$-2\alpha_s \Delta T_s K_{d,c} \frac{V_s}{V_c}.$$

By summing $\rho_{r,s}$ and $\rho_{r,\Sigma}$, the radial expansion reactivity is described as

$$\rho_r = 2\alpha_{support}\Delta T_{support}\left(K_R + K_{d,c}\frac{V_p + V_s}{V_c} - \left(K_{d,p} + K_{d,s}\right)\right) - 2\alpha_p \Delta T_p K_{d,c}\frac{V_p}{V_c} - 2\alpha_s \Delta T_s K_{d,c}\frac{V_s}{V_c}. \quad (24)$$

When the wrapper tube is the only structural material expanding outside the fuel pins, Eq. (24) becomes:

$$\rho_r = 2\alpha_{support}\Delta T_{support}\left(K_R + K_{d,c}\frac{V_p + V_s}{V_c} - \left(K_{d,p} + K_{d,s}\right)\right) - 2\alpha_p \Delta T_p K_{d,c}\frac{V_p}{V_c} - 2\alpha_{wr} \Delta T_{wr} K_{d,c}\frac{V_{wr}}{V_c}. \quad (25)$$

4 Differences from conventional formulas

The expansion reactivity calculation formulas for the fast reactor using oxide fuel are shown in a technical report [10]. Here, the differences between the calculation formulas shown in the report and that derived in the present study are discussed.

In the technical report [10], the formula for calculating z-axis expansion reactivity is expressed as

$$\rho_z = \left(K_H - K_{d,f}\right)\alpha_f \Delta T_f - K_{d,s}\alpha_s \frac{V_{cl}}{V_s}\Delta T_{cl} - K_{d,s}\alpha_s \frac{V_{wr}}{V_s}\Delta T_{wr}. \quad (26)$$

In Eq. (26), the expansion reactivity for both cladding and wrapper tubes is calculated using the density reactivity coefficient of structural materials. The contribution of cladding and wrapper tube are taken by using a proportion with the total volume. The

thermal expansion coefficients of the cladding and wrapper tubes are assumed to be the same as the structural materials. While Eq. (26) is suitable when cladding and wrapper tubes are made from the same material, Eq. (10) is more appropriate when their materials are different.

In the technical report [10], the formula for calculating the radial expansion reactivity can be expressed as

$$\rho_r = 2\alpha_{support}\Delta T_{support}\left(K_R + K_{d,c}\frac{V_p + V_s}{V_c} - \left(K_{d,p} + K_{d,s}\right)\right) - 2\alpha_s \Delta T_{cl} K_{d,c}\frac{V_p}{V_c} - 2\alpha_s \Delta T_{wr} K_{d,c}\frac{V_{wr}}{V_c}, \quad (27)$$

here, a coefficient 2 of the term containing K_R is not shown in the technical report [10], but is modified in the paper. In the second and third terms on the right side of Eq. (27), the thermal expansion coefficient used for considering the expansion of the fuel pin is the coefficient of the structural materials. It can be confirmed that previous study has represented the linear expansion coefficient of the pin using the coefficient of structural materials. On the other hand, in the present formula shown in Eq. (25), the radial expansion of the fuel pin is treated using a linear expansion coefficient α_p, which accounts for the expansion of both the fuel and the cladding.

5 Accuracy of Uniform Expansion Reactivity Evaluation Based on Reactivity Coefficients

This chapter discusses the accuracy of the evaluation results of expansion reactivity based on reactivity coefficients. The calculation condition and results are respectively shown in Section 5.1 and 5.2.

177

178 **5.1 Calculation Conditions**

179 **5.1.1 Expansion Ratio in Sodium-Cooled Fast Reactors**

180 In this paper, we consider the expansion of the fuel and the lower core support
181 structure. In a technical report for a sodium-cooled fast reactor with MOX fuel, formulas
182 for calculating thermal expansion coefficients are presented [10]. Figures 1(a) and 1(b)
183 show the thermal expansion coefficients for the structural material of the lower support
184 plate (SUS316) and the MOX fuel obtained from the calculation formulas presented in this
185 technical report. The boiling point of sodium is approximately 900°C, thus, Fig. 1(a) shows
186 that the thermal expansion coefficient of the lower support plate is less than 2.2×10^{-5}/K.
187 Therefore, even if the sodium temperature increases by 100°C, the expansion ratio
188 remains below 2.2E-3, which is less than 1%. Additionally, Fig. 1(b) indicates that the
189 thermal expansion coefficient is below 2.2×10^{-5}/K even at around 2400°C, which is near
190 the melting point of MOX fuel. As for metallic fuels, the average thermal expansion
191 coefficient for U-Pu-Zr alloys is reported to be 1.7×10^{-5} /K [14,15]. Therefore, for the MOX
192 fuel or U-Pu-Zr alloys used as metallic fuels, even if the fuel temperature increases by
193 500°C, the expansion ratio would be around 1% or less. In this paper, assuming large
194 temperature changes, the accuracy of expansion reactivity for expansion ratios of up to
195 2% is discussed.

196

197 **5.1.2 Core Geometry and Calculation Method**

Two simplified core geometries (Core A and B) with varying core height to diameter ratio were used (Fig. 2). The fuel region is based on the inner fuel specifications of the Monju [7]. To obtain the 70-group cross-sections based on JENDL-4.0 [16], a pin-cell calculation is performed using SLAROM-UF [17]. Using the 70-group macroscopic cross-sections for the MOX fuel, SUS316, and sodium obtained from the pin-cell calculation, the homogenized 70-group cross-sections for the fuel assembly are calculated. The calculation condition for the 70-group macroscopic cross-sections is the same as that used in the transient calculation for Monju [7]. The homogenized cross section was calculated using volume weighting. For more precise calculations, it would be appropriate to use the flux-volume-weighted homogenized cross section, which accounts for the neutron flux distribution within the assembly. Since this study is not aimed at precisely determining core characteristics but rather focuses on discussing the approximation error of the expansion reactivity, the volume-weighted cross section was used for the calculation.

The core calculations are performed using CITATION based on diffusion theory. The calculations are carried out in an R-Z geometry with 100 divisions in both the radial and Z-axis directions of the fuel region. The convergence criteria are set to 5×10^{-4} for the neutron flux in each region and 1×10^{-6} for the multiplication factor. The boundary condition is set to vacuum. Using CITATION, the reactivity coefficients presented in Sections 2 and 3 are calculated. Then, the Z-axis and radial expansion reactivities are obtained using the volumes of each material (e.g., coolant) in the Monju. In this calculation, the density reactivity coefficient (e.g., $K_{d,f}$) and reactivity coefficient due to shape changes (e.g., K_H) are obtained using 1% expansion in the axial or radial directions.

The expansion reactivity obtained from the reactivity coefficients is compared to the expansion reactivity directly calculated by expanding the geometry in CITATION.

5.2 Numerical Results

5.2.1 Z-axis Expansion Reactivity

As mentioned in Section 2, the reactivity introduced by the thermal expansion of the wrapper tube in the Z-axis direction is small. Therefore, in this section, we discuss the reactivity obtained using the formulas derived in Section 2, considering two cases: when only the fuel expands and when both the fuel and cladding expand. Figure 3(a) compares reactivity for Core A with only fuel expansion, while Figure 3(b) includes both fuel and cladding expansion. As shown in Fig. 3, the reactivity due to Z-axis expansion shows approximately linear behavior within the expansion range of 0 to 2%. This indicates that interpolation and extrapolation of reactivity using the reactivity coefficients are justified. Additionally, the difference between the reactivity calculated using reactivity coefficients and the direct calculation is within a few percent. Figure 4 shows a comparison of Z-axis expansion reactivity for Core B. The magnitude of axial reactivity is smaller than Core A since Core B is flatter than Core A. Similar to Core A, the reactivity in Core B also shows linear behavior, and the difference between the reactivity calculated using reactivity coefficients and the direct calculation closely matches, being within a few percent. These results show that Z-axis expansion reactivity can be accurately estimated using the derived formulas.

For Monju, since the cladding and wrapper tubes are made of the same material, the z-axis expansion reactivity is identical between the present formulas and the conventional formulas.

5.2.2 Radial Expansion Reactivity

In our previous study [11], it was confirmed that changes in the amount of sodium within the core before and after expansion have a relatively small impact on expansion reactivity. Therefore, for radial expansion, we focus on the reactivity introduced by the expansion of the lower core support plate. Figures 5 and 6 show comparisons of radial expansion reactivity for Core A and Core B, respectively. Compared to Core A, the magnitude of radial reactivity is larger for Core B. For both core geometries, the reactivity due to radial expansion shows approximately linear behavior within the expansion range of 0 to 2%. Additionally, the difference between the reactivity calculated using reactivity coefficients and the direct calculation is within a few percent. These results demonstrate that the radial expansion reactivity can also be accurately estimated using the derived formulas.

Next, let us discuss the reactivity difference between the present and conventional formulas. One major difference is that the conventional formulas do not consider the expansion of the fuel in the term related to fuel pin expansion. Table 1 shows a comparison of the radial expansion reactivity obtained using the conventional formulas and the present formulas when the radial expansion ratio is 1%. To simplify the discussion, the interaction between the fuel and the cladding was ignored in the calculation. These

results confirm that even at a 1% expansion of the fuel, the difference between the present and conventional formulas is about 3×10^{-5} $\Delta k/kk'$ or less.

6 Conclusion and future work

In this study, to evaluate the uniform axial and radial expansion reactivity in sodium-cooled fast reactors with low computational cost, we derived an evaluation formula based on reactivity coefficients and confirmed the accuracy. For axial expansion, the expansion of fuel, cladding, and wrapper tubes are considered. For radial expansion, the expansion of the fuel pin, lower core support plate, and structural materials are considered. In these derivations, the expansion reactivity is divided into the shape change effect and the macroscopic cross-section change effect, and these effects are expressed by the reactivity coefficients of materials in the core.

We compared the derived formulas with conventional formulas. While the formulas are generally consistent, there are some differences in some expressions. To confirm the accuracy of the proposed formulas, numerical calculations were performed using two different core geometries (Core A and Core B). Reactivities due to Z-axis and radial expansions were calculated using both the reactivity coefficients and direct calculation considering core expansion. As a result, for the expansion range of 0 to 2%, the differences between the reactivity calculated using the reactivity coefficients and the direct calculation were within a few percent. For both Z-axis and radial expansions, the reactivity changes show linear behavior within the expansion range, demonstrating that interpolation and extrapolation using the reactivity coefficients are feasible.

285 This study assumes uniform expansion in both radial and axial directions. However,
286 during transient conditions in fast reactors, non-uniform expansion, such as fuel assembly
287 bowing, can also occur. Future work is expected to develop methods that can be applied
288 to such non-uniform expansions.
289
290

References

[1] Fuchita, S., Fujimura, K., Fujimata, K., Takeda, S., and Takeda, T., 2020, "Development of safety-enhanced fast reactor by using minor actinide bearing internal blanket," Proceedings of the 2020 International Conference on Nuclear Engineering (ICONE2020). https://doi.org/10.1115/ICONE2020-16746

[2] Shimamoto, Y., Kitada, T., Takeda, S., Okita, T., and Hoashi, E., 2023, "Design range of Fast Reactor with Inherent Safety for Effective Transmutation of Minor Actinide: 1. Screening with constraint of negative void reactivity," Proceedings of the 30th International Conference on Nuclear Engineering (ICONE30). https://doi.org/10.1299/jsmeicone.2023.30.1760

[3] Okita, T., Hoashi, E., Shimamoto, Y., Takeda, S., and Kitada, T., 2023, "Design range of Fast Reactor with Inherent Safety for Effective Transmutation of Minor Actinide: 2. Verification of heat removal via natural convection in core region," Proceedings of the 30th International Conference on Nuclear Engineering (ICONE30). https://doi.org/10.1299/jsmeicone.2023.30.1926

[4] Okita, T., Takeda, S., Hoashi, E., and Kitada, T., 2023, "Fundamental design activity of fast reactor with inherent safety characteristics for effective transmutation of minor actinide," Mechanical Engineering Journal, 11(2), 23-00494. https://doi.org/10.1299/mej.23-00494

[5] Takeda, T., Fujimura, K., Fujimata, K., and Takeda, S., 2018, "Effect of void propagation to sodium void reactivity in transient analyses of fast reactors with

312 sodium-plenum," Annals of Nuclear Energy, 119, pp. 175-179.
313 https://doi.org/10.1016/j.anucene.2018.05.007
314 [6] Fujimura, K., Fuchita, S., Fujimata, K., and Takeda, S., 2023, "A safety enhanced
315 sodium-cooled MOX fueled fast reactor core concept," Journal of Nuclear Science
316 and Technology, 60(10), pp. 1258-1269.
317 https://doi.org/10.1080/00223131.2023.2188268
318 [7] Takeda, S., Takeda, T., Fuchita, S., and Kitada, T., 2020, "Development of an improved
319 quasi-static transient analysis code based on three-dimensional Sn nodal transport
320 theory for fast reactor," Annals of Nuclear Energy, 143, 107499.
321 https://doi.org/10.1016/j.anucene.2020.107499
322 [8] Jing, T., and Yang, W. S., 2019, "Development of the RAINBOW code to evaluate
323 assembly bowing reactivity coefficients in sodium-cooled fast reactors," Annals of
324 Nuclear Energy, 129, pp. 289-297. https://doi.org/10.1016/j.anucene.2019.02.004
325 [9] Wang, Y., Chen, J., Wei, L., Yin, H., Zheng, Y., and Du, X., 2021, "A method for
326 calculating the assembly bowing reactivity coefficients in sodium fast reactor,"
327 Annals of Nuclear Energy, 155, 108176.
328 https://doi.org/10.1016/j.anucene.2021.108176
329 [10] Takashita, H., Higuchi, M., Togashi, N., and Hayashi, T., 2000, "Report on neutronic
330 design calculational methods," Japan Nuclear Cycle Development Institute, JNC-
331 TN8410 2000-011. [in Japanese]. URL: https://jopss.jaea.go.jp/pdfdata/JNC-TN8410-
332 2000-011.pdf

[11] Takeda, S., Kitada, T., Okita, T., and Hoashi, E., 2024, "Evaluation of expansion reactivity based on reactivity coefficient for sodium-cooled fast reactor," Proceedings of the 31th International Conference on Nuclear Engineering (ICONE31), Prague, Czech Republic, August 4-8, 2024, ICONE31-132277.

[12] Nagaya, Y., Okumura, K., Sakurai, T., and Mori, T. M., 2017, "MVP/GMVP Version 3: General Purpose Monte Carlo Codes for Neutron and Photon Transport Calculations Based on Continuous Energy and Multigroup Methods," JAEA-Data/Code 2016-018.

[13] Fowler, T. B., Vondy, D. R., and Cunningham, G. W., 1971, "Nuclear Reactor Core Analysis Code: CITATION," USAEC Report ORNL-TM-2496, Rev. 2, ORNL, Oak Ridge, Tennessee, USA.

[14] Shaw, A., Bostelmann, F., Hartanto, D., Walker, E., and Wieselquist, W. A., 2023, "SCALE Modeling of the Sodium Cooled Fast-Spectrum Advanced Burner Test Reactor," Oak Ridge National Laboratory, ORNL/TM-2022/2758. https://doi.org/10.2172/1991734

[15] Janney, D. E., 2017, "Metallic Fuels Handbook, Part 1: Alloys Based on U-Zr, Pu-Zr, U-Pu, or U-Pu-Zr, Including Those with Minor Actinides (Np, Am, Cm), Rare-earth Elements (La, Ce, Pr, Nd, Gd), and Y," Technical Report INL/EXT-15-36520, Idaho National Laboratory, Idaho Falls, ID. https://doi.org/10.2172/1504934

[16] Shibata, K., Iwamoto, O., Nakagawa, T., Iwamoto, N., Ichihara, A., Kunieda, S., Chiba, S., Furutaka, K., Otuka, N., Ohsawa, T., Murata, T., Matsunobu, H., Zukeran, A., Kamada, S., and Katakura, J., 2011, "JENDL-4.0: A New Library for Nuclear Science

and Engineering," Journal of Nuclear Science and Technology, 48(1), pp. 1-30. https://doi.org/10.1080/18811248.2011.9711675

[17] Hazama, T., Chiba, G., and Sugino, K., 2012, "Development of a Fine and Ultra-Fine Group Cell Calculation Code SLAROM-UF for Fast Reactor Analyses," Journal of Nuclear Science and Technology, 43(8), pp. 908-918. https://doi.org/10.1080/18811248.2006.9711176

363 **Figure Captions List**
364

365

366

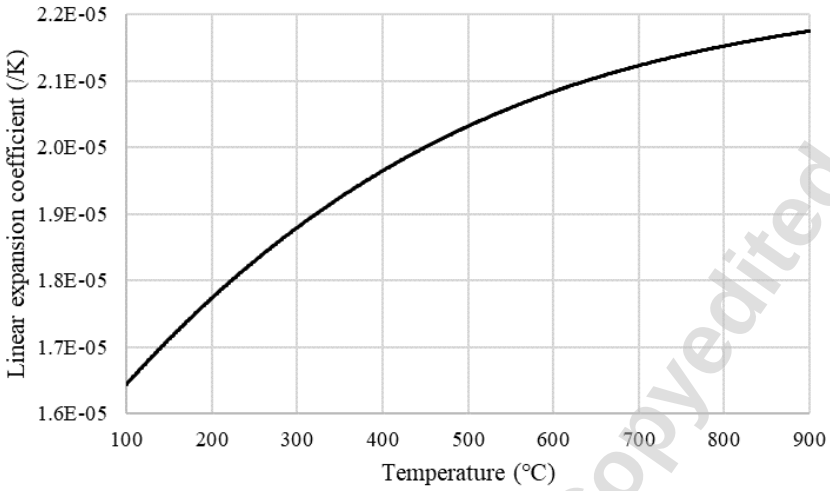

367
368 (a) SUS316

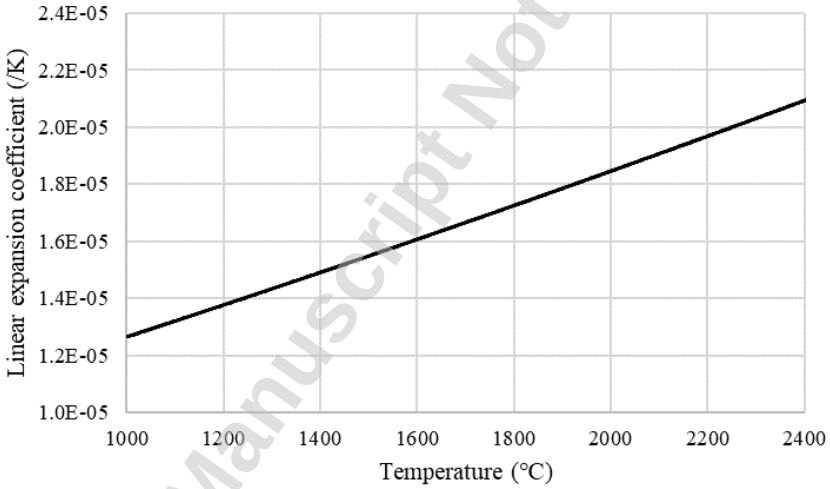

369
370 (b) MOX fuel
371 Fig. 1 Thermal expansion coefficient

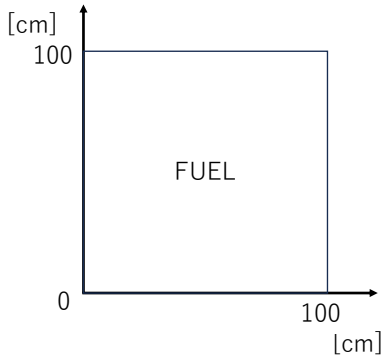

(a) Core A

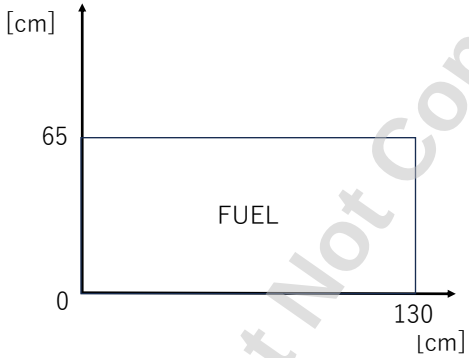

(b) Core B

Fig. 2 Simple core geometry

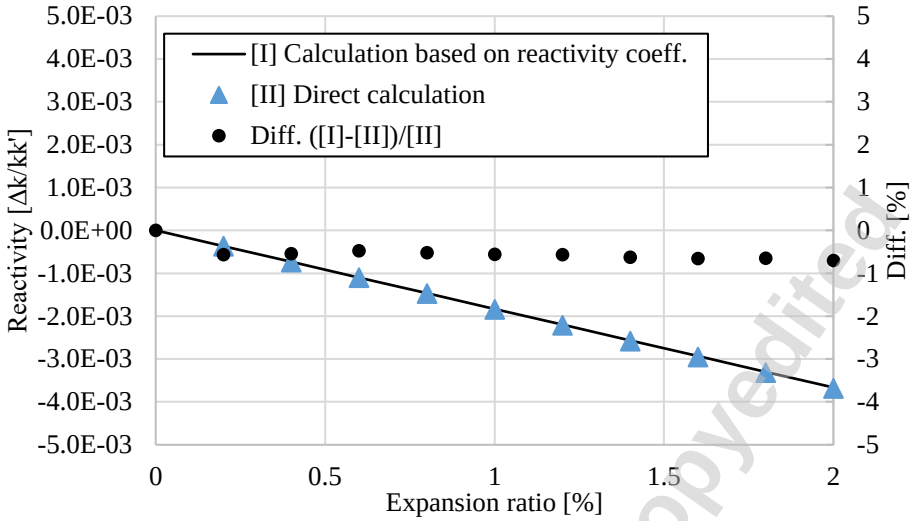

(a) Fuel expansion only

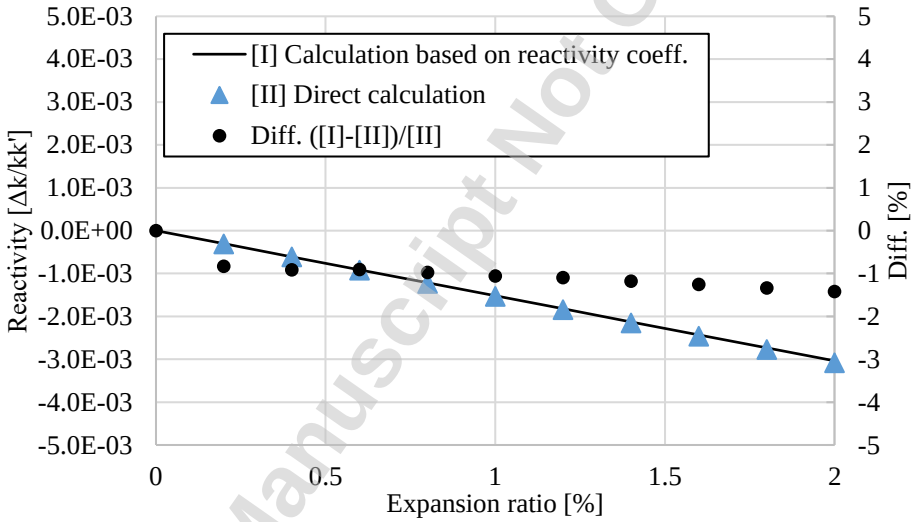

(b) Fuel and cladding Expansion

Fig. 3 Comparison of Z-axis expansion reactivity for Core A

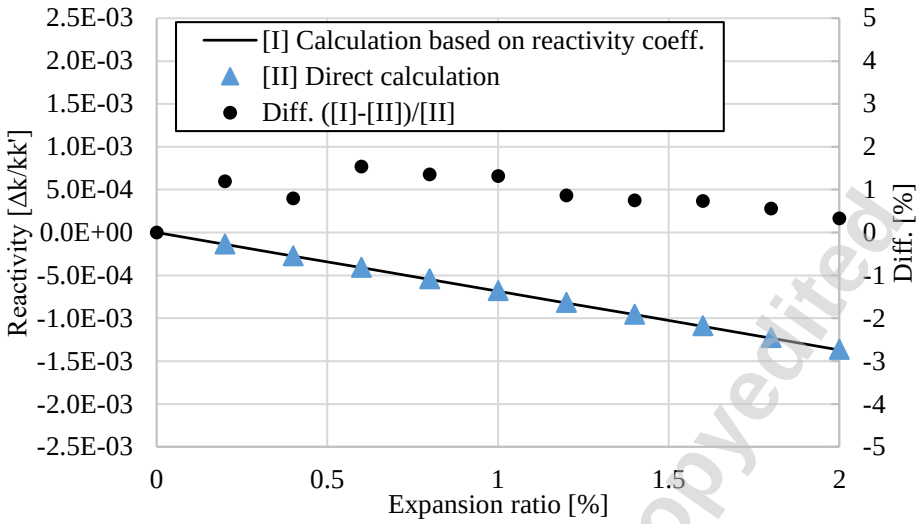

(a) Fuel expansion only

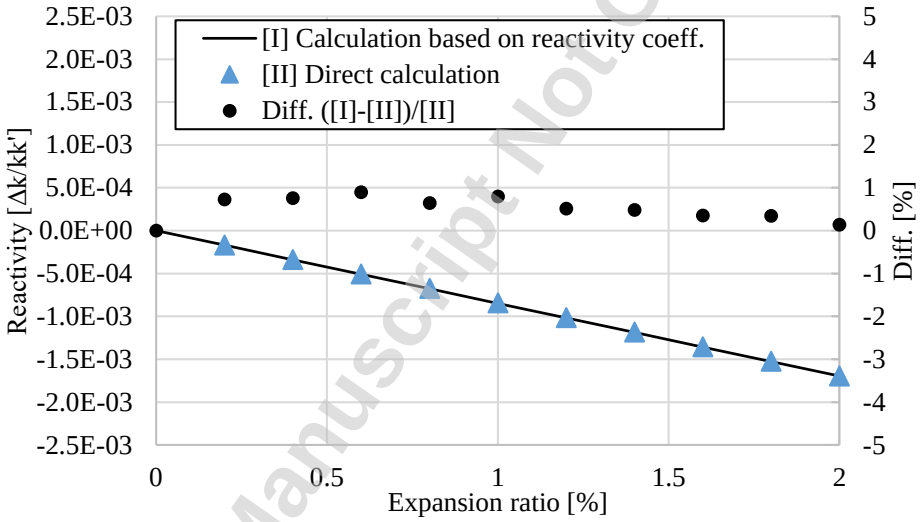

(b) Fuel and cladding Expansion

Fig. 4 Comparison of Z-axis expansion reactivity for Core B

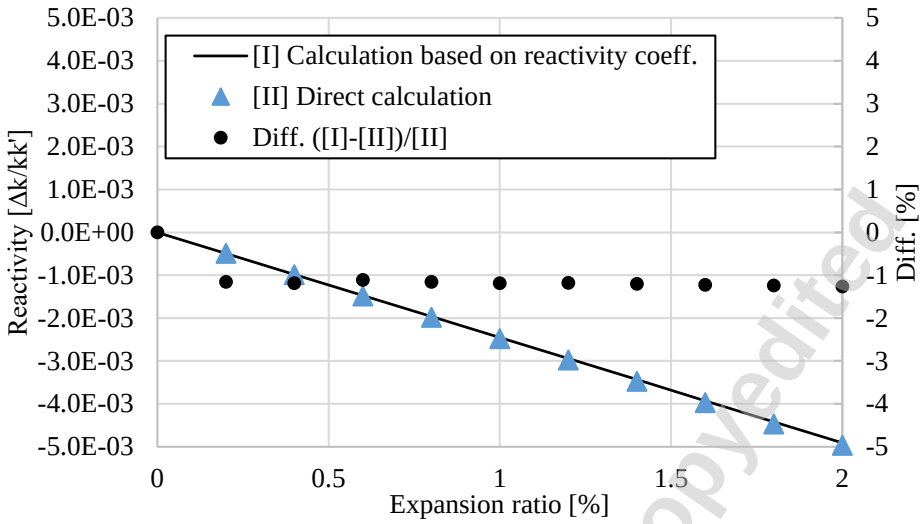

Fig. 5 Comparison of radial expansion reactivity for Core A

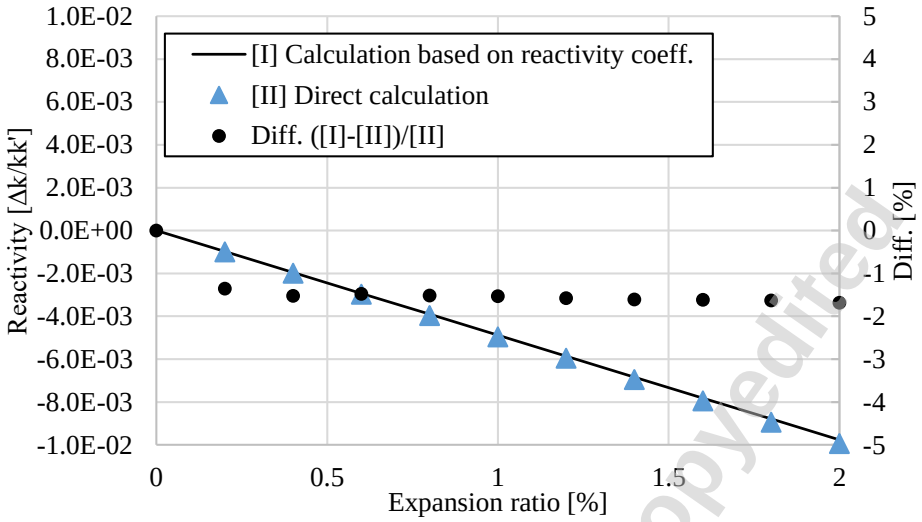

Fig. 6 Comparison of radial expansion reactivity for Core B

392 **Table Caption List**
393

Table 1 Comparison of radial expansion reactivity.

394
395

396 Table 1 Comparison of radial expansion reactivity.

Core geometry	(i) Present formulas [Δk/kk']	(ii) Conventional formulas [Δk/kk']	(i) -(ii) [Δk/kk']
Core A	-2.3×10^{-4}	-2.4×10^{-4}	0.1×10^{-4}
Core B	-5.4×10^{-4}	-5.1×10^{-4}	-0.3×10^{-4}

397